Hybrid magnetic attitude control gain selection

C J Damaren

Proceedings of the Institution of Mechanical Engineers, Part G: Journal of Aerospace Engineering 2009 223: 1041
DOI: 10.1243/09544100JAERO641

Hybrid magnetic attitude control gain selection

C J Damaren
Institute for Aerospace Studies, University of Toronto, 4925 Dufferin Street, Toronto, Ontario M3H 5T6, Canada
email: damaren@utias.utoronto.ca

The manuscript was received on 8 June 2009 and was accepted after revision for publication on 13 July 2009.

DOI: 10.1243/09544100JAERO641

Abstract: For spacecraft in low Earth orbits, attitude control via the torques provided by the geomagnetic field is an attractive option. Recent research has demonstrated that asymptotic pointing of attitude setpoints is possible using a linear combination of Euler parameter and angular velocity feedback. However, given the time-varying nature of the magnetic field, the size of the gains leading to stability is restricted. The present work looks at a hybrid scheme consisting of magnetic control using on-board dipole moments and an independent three-axis actuation scheme (i.e. reaction wheels or thrusters). A stability analysis is presented using passivity concepts that shows that the limitation on magnetic control gains can be removed if a minimum level of three-axis actuation augments the magnetic scheme.

Keywords: magnetic attitude control, passivity theorem

1 INTRODUCTION

The primary disturbance torques acting on spacecraft in geocentric orbits are those due to aerodynamics, the geomagnetic field, gravity gradient, and solar-radiation pressure. In each case, these can also be harnessed for attitude control purposes. In particular, the torque produced by the geomagnetic field interacting with on-board magnetic dipole moments (created by current-carrying coils) can be used to produce a control torque. There are interesting controllability issues associated with this torque since it originates from a cross-product law involving the previous two quantities. However, since the direction of the magnetic field is usually changing, the pointwise uncontrollable direction is also changing. A recent survey of magnetic spacecraft attitude control is presented in reference [**1**].

Recent work by Lovera and Astolfi [**2**, **3**] addressed the regulation of attitude setpoints using the geomagnetic torque. They examined proportional–derivative (PD) control using Euler parameters (quaternions) and the angular velocity. It is well known [**4**] that a linear combination of these variables in the case of full three-axis actuation (such as can be provided by reaction wheels or thrusters) renders the spacecraft attitude and rate globally asymptotically stable. In references [**2**] and [**3**], the corresponding extension to magnetic attitude control requires that the average of a certain matrix involving the geomagnetic field be positive definite. In this case, there are limitations on the size of the PD gains given the time-varying nature of the magnetic field. This in turn limits the settling time for attitude regulation.

Many spacecraft carry magnetic torquers as well as an alternative three-axis actuation system such as reaction wheels or thrusters. The magnetic torquers can be used for detumbling and momentum dumping of the reaction wheels. In some cases, it may be beneficial to simultaneously use the magnetic actuation system in concert with the three-axis system. This shall be termed hybrid magnetic attitude control. For example, this can extend the torquing capability of the spacecraft and may have beneficial repercussions on power consumption. A natural question to ask is, to what extent can the three-axis capability mitigate the gain limitations on the magnetic actuation system?

In this article, the hybrid attitude control problem is formulated and a stability analysis on the linearized system is performed. The feedback control structure combines the PD law of reference [**3**] for the magnetic dipole moments with a three-axis PD law. The present author's primary analysis tool is passivity and bounds on the feedback gains are established that lead to a locally asymptotically stable system. Simulation results are used to validate the analysis.

2 SPACECRAFT ATTITUDE DYNAMICS

The rotational dynamics of a rigid-body spacecraft can be modelled using Euler's equation

$$\mathbf{I}\dot{\boldsymbol{\omega}} + \boldsymbol{\omega}^{\times}\mathbf{I}\boldsymbol{\omega} = \boldsymbol{d} + \boldsymbol{m}^{\times}\boldsymbol{B}_{\mathrm{b}} + \boldsymbol{u} \tag{1}$$

where $\mathbf{I}$ is the moment of inertia matrix, $\boldsymbol{\omega}$ is the angular velocity expressed in a body-fixed frame, $\boldsymbol{d}$ is the disturbance torque, and

$$\boldsymbol{\omega}^{\times} = \begin{bmatrix} 0 & -\omega_3 & \omega_2 \\ \omega_3 & 0 & -\omega_1 \\ -\omega_2 & \omega_1 & 0 \end{bmatrix}$$

In equation (1) are introduced the torque produced by the three-axis actuation system, $\boldsymbol{u}$, and the dipole moment used for magnetic control, $\boldsymbol{m}$. The quantity $\boldsymbol{B}_{\mathrm{b}}$ contains the body-frame components of the geomagnetic field vector.

The attitude is modelled using the Euler parameters [**5**] (quaternions) $\boldsymbol{q} = [q_1\, q_2\, q_3]^{\mathrm{T}}$ and q_4. Defining $\bar{\boldsymbol{q}} = [q_1\, q_2\, q_3\, q_4]^{\mathrm{T}}$, they satisfy the kinematical equation

$$\dot{\bar{\boldsymbol{q}}} = \frac{1}{2}\mathbf{Q}(\bar{\boldsymbol{q}})\omega, \quad \mathbf{Q}(\bar{\boldsymbol{q}}) = \begin{bmatrix} q_4\mathbf{1} + \boldsymbol{q}^{\times} \\ -\boldsymbol{q}^{\mathrm{T}} \end{bmatrix} \tag{2}$$

The rotation matrix relating the inertial frame to the body frame can be computed from the quaternions using

$$\mathbf{C}_{\mathrm{bi}} = (q_4^2 - \boldsymbol{q}^{\mathrm{T}}\boldsymbol{q})\mathbf{1} + 2\boldsymbol{q}\boldsymbol{q}^{\mathrm{T}} - 2q_4\boldsymbol{q}^{\times} \tag{3}$$

It will maintain its orthogonality if the constraint $\bar{\boldsymbol{q}}^{\mathrm{T}}\bar{\boldsymbol{q}} = 1$ is maintained. The inertial frame has been identified as the target attitude for the body frame (i.e. $\boldsymbol{q} = \mathbf{0}$).

The magnetic field components satisfy $\boldsymbol{B}_{\mathrm{b}} = \mathbf{C}_{\mathrm{bi}}\boldsymbol{B}_{\mathrm{i}}$, where the inertial frame components $\boldsymbol{B}_{\mathrm{i}}$ will be modelled using a tilted dipole model [**6**]. It is also assumed that the inertial frame corresponding to the desired attitude is the geocentric inertial frame. Therefore

$$\boldsymbol{B}_{\mathrm{i}} = \begin{bmatrix} (B_r\cos\delta + B_\theta\sin\delta)\cos\alpha - B_\phi\sin\alpha \\ (B_r\cos\delta + B_\theta\sin\delta)\sin\alpha + B_\phi\cos\alpha \\ B_r\sin\delta - B_\theta\cos\delta \end{bmatrix}$$

where α and δ are the spacecraft right ascension and declination. From them, it is possible to calculate ϕ_m, the east longitude, and θ_m, the coelevation. B_r, B_θ, B_ϕ are the geomagnetic field components in spherical coordinates and are given as follows

$$B_r = 2\left(\frac{R_{\mathrm{e}}}{R_{\mathrm{b}}}\right)^3 [g_1^0\cos\theta_m + (g_1^1\cos\phi_m + h_1^1\sin\phi_m)\sin\theta_m]$$

$$B_\theta = \left(\frac{R_{\mathrm{e}}}{R_{\mathrm{b}}}\right)^3 [g_1^0\sin\theta_m - (g_1^1\cos\phi_m + h_1^1\sin\phi_m)\cos\theta_m]$$

$$B_\phi = \left(\frac{R_{\mathrm{e}}}{R_{\mathrm{b}}}\right)^3 [g_1^1\sin\phi_m - h_1^1\cos\phi_m]$$

where R_{e} is the Earth's mean equatorial radius, R_{b} is the spacecraft position, and the coefficients g_1^0, g_1^1, and h_1^1 are taken from the 1995 International Geomagnetic Reference Field

$$g_1^0 = -29\,682\,\mathrm{nT}, \quad g_1^1 = -1789\,\mathrm{nT}, \quad h_1^1 = 5310\,\mathrm{nT}$$

In the sequel, the present author wishes to develop feedback controllers that regulate the spacecraft about the equilibrium (if $\boldsymbol{d}$ is neglected) $\boldsymbol{\omega} = \boldsymbol{q} = \mathbf{0}$.

3 CONTROL SYSTEM MODEL

For the three-axis actuation system, it is assumed that the torques are generated according to the control law

$$\boldsymbol{u}(t) = -\gamma\mathbf{I}^{-1}[\epsilon k_{\mathrm{d}}\boldsymbol{\omega}(t) + 2\epsilon^2 k_{\mathrm{p}}\boldsymbol{q}(t)] \tag{4}$$

The stability properties of this control law in the absence of the magnetic controller are given by the following lemma.

Lemma 1

For $\boldsymbol{m} = \boldsymbol{d} = \mathbf{0}$ and $\gamma > 0$, $k_{\mathrm{d}} > 0$, $k_p > 0$, $\epsilon > 0$, the equilibrium $\boldsymbol{\omega} = \boldsymbol{q} = \mathbf{0}$ of equations (1), (2), and (4) is globally asymptotically stable.

Proof

This follows simply from the use of the Lyapunov function [**7**]

$$V = \frac{1}{2}\boldsymbol{\omega}^{\mathrm{T}}\mathbf{I}^2\boldsymbol{\omega} + 2\gamma\epsilon^2 k_{\mathrm{p}}[\boldsymbol{q}^{\mathrm{T}}\boldsymbol{q} + (q_4 - 1)^2]$$

followed by the application of LaSalle's theorem.

Following reference [**3**], the following control law for the magnetic control dipole moment is adopted

$$\begin{aligned} \boldsymbol{m}(t) &= \|\boldsymbol{B}_{\mathrm{i}}(t)\|^{-2}\boldsymbol{B}_{\mathrm{b}}^{\times}(t)\boldsymbol{v}(t) \\ \boldsymbol{v}(t) &= -\mathbf{I}^{-1}[\epsilon k_{\mathrm{d}}\boldsymbol{\omega}(t) + 2\epsilon^2 k_{\mathrm{p}}\boldsymbol{q}(t)] \end{aligned} \tag{5}$$

The use of the redundant parameter ϵ parallels its use in references [**2**] and [**3**] where it plays an important role in stability proofs using averaging theory. It has been used here so that lemma 2 and its proof may be employed. The parameter ϵ has also been used in the three-axis control law in equation (4) so that γ can be used as a pure dimensionless scaling. As will be demonstrated, it is a rough measure of the relative size of the three-axis torques and those provided by the magnetic coils.

The stability properties of equation (5) in the absence of the three-axis actuation torque are governed by the following lemma.

Lemma 2

Let $\boldsymbol{d} = \boldsymbol{u} = \mathbf{0}$ in equation (1). Assume that the spacecraft orbit is such that

$$\bar{\boldsymbol{\Gamma}}_0 = \lim_{T\longrightarrow\infty} -\frac{1}{T}\int_0^T \|\boldsymbol{B}_\mathrm{i}(t)\|^{-2}\boldsymbol{B}_\mathrm{i}^\times(t)\boldsymbol{B}_\mathrm{i}^\times(t)\,\mathrm{d}t > \mathbf{O} \qquad (6)$$

Then, for given finite gains $k_\mathrm{p} > 0$, $k_\mathrm{d} > 0$, there exists $\epsilon^* > 0$ such that for any $0 < \epsilon < \epsilon^*$, the equilibrium $\boldsymbol{\omega} = \boldsymbol{q} = \mathbf{0}$ of equations (1), (2), and (5) is locally exponentially stable.

Proof

See reference [**3**].

The lemma places clear bounds on the size of the gains leading to a sufficient condition for stability. Note that ϵ^* is a decreasing function of k_p and k_d. It is not hard to construct numerical examples where larger gains lead to instability. This will be demonstrated in section 4. Unfortunately the lemma provides no constructive way of determining ϵ^* and it must essentially be determined by online tuning using simulation. It was an attempt to quantify ϵ^* that led to the present article.

Let us now examine the simultaneous application of the torques described by equations (4) and (5). In preparation for the stability analysis, equations (1) to (5) are linearized. Assume that the body frame differs from the inertial frame by small angles $\boldsymbol{\theta} = 2\boldsymbol{q}$, i.e. $\mathbf{C}_\mathrm{bi} = \mathbf{1} - \boldsymbol{\theta}^\times$, and small rates $\boldsymbol{\omega} = \dot{\boldsymbol{\theta}}$. Making these substitutions in equations (1), (4), and (5) while neglecting products of small terms leads to the linearized motion equation

$$\mathbf{I}\ddot{\boldsymbol{\theta}} = (\tilde{\boldsymbol{B}}_\mathrm{i}^\times\tilde{\boldsymbol{B}}_\mathrm{i}^\times - \gamma\mathbf{1})\mathbf{I}^{-1}(\epsilon k_\mathrm{d}\dot{\boldsymbol{\theta}} + \epsilon^2 k_\mathrm{p}\boldsymbol{\theta}) + \boldsymbol{d}$$

or

$$\ddot{\boldsymbol{\theta}} + (\gamma\mathbf{I}^{-2} - \mathbf{I}^{-1}\tilde{\boldsymbol{B}}_\mathrm{i}^\times\tilde{\boldsymbol{B}}_\mathrm{i}^\times\mathbf{I}^{-1})(\epsilon k_\mathrm{d}\dot{\boldsymbol{\theta}} + \epsilon^2 k_\mathrm{p}\boldsymbol{\theta}) = \mathbf{I}^{-1}\boldsymbol{d} \qquad (7)$$

where $\tilde{\boldsymbol{B}}_\mathrm{i} = \|\boldsymbol{B}_\mathrm{i}\|^{-1}\boldsymbol{B}_\mathrm{i}$. Note that $\boldsymbol{B}_\mathrm{i}$ is used instead of $\boldsymbol{B}_\mathrm{b}$ in equation (7) because linearized equations for the stability analysis are desired. Note that under a small attitude angle approximation $\boldsymbol{B}_\mathrm{b} = (\mathbf{1} - \boldsymbol{\theta}^\times)\boldsymbol{B}_\mathrm{i}$. If this is inserted into the motion equations, the term containing $\boldsymbol{\theta}^\times$ leads to products of small angles and products of small angles and rates that can be neglected in the linear stability analysis.

Note that sensor noises may be incorporated into the analysis by replacing $\boldsymbol{\theta}$ with $\boldsymbol{\theta} + \mathbf{n}_1$ and $\dot{\boldsymbol{\theta}}$ with $\dot{\boldsymbol{\theta}} + \mathbf{n}_2$. This leads to a modification of equation (7) in which $\boldsymbol{d}$ is replaced with $\hat{\boldsymbol{d}} = \boldsymbol{d} + \mathbf{N}\mathbf{n}$ where $\mathbf{n} = [\mathbf{n}_1^\mathrm{T}\ \ \mathbf{n}_2^\mathrm{T}]^\mathrm{T}$ contains the sensor noises and $\mathbf{N} = [\tilde{\boldsymbol{B}}_\mathrm{b}^\times\tilde{\boldsymbol{B}}_\mathrm{b}^\times - \gamma\mathbf{1}]\mathbf{I}^{-1}[\epsilon^2 k_\mathrm{p}\mathbf{1}\ \ \epsilon k_\mathrm{d}\mathbf{1}]$ with $\tilde{\boldsymbol{B}}_\mathrm{b} = \|\boldsymbol{B}_\mathrm{b}\|^{-1}\boldsymbol{B}_\mathrm{b}$.

Now introduce the eigendecomposition of the inertia matrix, $\mathbf{I} = \mathbf{E}\boldsymbol{\Lambda}\mathbf{E}^\mathrm{T}$, where $\mathbf{E}$ is the orthogonal eigenmatrix and $\boldsymbol{\Lambda} = \mathrm{diag}\{\lambda_1, \lambda_2, \lambda_3\}$ is the diagonal matrix of principal moments of inertia (eigenvalues). Letting $\boldsymbol{\theta}(t) = \mathbf{E}\boldsymbol{\psi}(t)$ in equation (7) and substituting the eigendecomposition for $\mathbf{I}$ leads to

$$\ddot{\boldsymbol{\psi}} + [\gamma\boldsymbol{\Lambda}^{-2} + \Xi(t)][\epsilon k_\mathrm{d}\dot{\boldsymbol{\psi}} + \epsilon^2 k_\mathrm{p}\boldsymbol{\psi}] = \mathbf{E}^\mathrm{T}\mathbf{I}^{-1}\hat{\boldsymbol{d}} \qquad (8)$$

where

$$\Xi(t) = -\mathbf{E}^\mathrm{T}\mathbf{I}^{-1}\tilde{\boldsymbol{B}}_\mathrm{i}^\times(t)\tilde{\boldsymbol{B}}_\mathrm{i}^\times(t)\mathbf{I}^{-1}\mathbf{E} = \Xi^\mathrm{T}(t) \geqslant \mathbf{O} \qquad (9)$$

Let us define

$$\boldsymbol{y} = \epsilon k_\mathrm{d}\dot{\boldsymbol{\psi}} + \epsilon^2 k_\mathrm{p}\boldsymbol{\psi}$$

The mapping from $\hat{\boldsymbol{d}}$ to $\boldsymbol{y}$ is shown in the form of a block diagram in Fig. 1. It has been represented as the feedback interconnection of two operators $\boldsymbol{G}$ and $\boldsymbol{H}$. Since $\boldsymbol{G}$ is linear time-invariant (LTI), it has been represented using Laplace transforms where s is the Laplace transform variable.

Now, it is necessary to establish conditions on the feedback gains that lead to stability of the linear time-varying system depicted in Fig. 1. The major tool used is the passivity theorem [**8**]. Prior to stating it, let us define a few fundamental notions. A function of time $\boldsymbol{y} \in L_2$ if $\int_0^\infty \boldsymbol{y}^\mathrm{T}(t)\boldsymbol{y}(t)\,\mathrm{d}t < \infty$. A function of time $\boldsymbol{y} \in L_{2e}$ if $\int_0^T \boldsymbol{y}^\mathrm{T}(t)\boldsymbol{y}(t)\,\mathrm{d}t < \infty$, $0 < T < \infty$. The system in Fig. 1 is L_2-stable if $\boldsymbol{d}, \mathbf{n} \in L_2 \Rightarrow \mathbf{E}^\mathrm{T}\mathbf{I}^{-1}\hat{\boldsymbol{d}} \in L_2 \Rightarrow \mathbf{y} \in L_2$. Note that since the multiplication operator $\mathbf{N}$ has finite gain, $\boldsymbol{d}, \mathbf{n} \in L_2 \Rightarrow \hat{\boldsymbol{d}} \in L_2$.

The operator $\boldsymbol{G}$ is passive if

$$\int_0^T \boldsymbol{\nu}^\mathrm{T}\boldsymbol{G}\boldsymbol{\nu}\,\mathrm{d}t \geqslant 0, \quad \forall T \geqslant 0, \quad \forall\boldsymbol{\nu} \in L_{2e}$$

The operator $\boldsymbol{H}$ is strictly passive if

$$\int_0^T \boldsymbol{y}^\mathrm{T}\boldsymbol{H}\boldsymbol{y}\,\mathrm{d}t \geqslant \varepsilon\int_0^T \boldsymbol{y}^\mathrm{T}\boldsymbol{y}\,\mathrm{d}t, \quad \forall T \geqslant 0, \quad \forall\boldsymbol{y} \in L_{2e}$$

for some $\varepsilon > 0$. The operator $\boldsymbol{H}$ in Fig. 1 is clearly strictly passive since it corresponds to multiplication

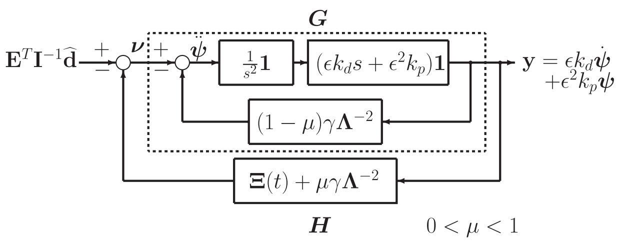

Fig. 1 Block diagram

by a positive-definite (but time-varying) matrix, that is

$$\int_0^T \boldsymbol{y}^{\mathrm{T}} \boldsymbol{H} \boldsymbol{y}\, \mathrm{d}t = \int_0^T \boldsymbol{y}^{\mathrm{T}} [\boldsymbol{\Xi}(t) + \mu\gamma \boldsymbol{\Lambda}^{-2}] \boldsymbol{y}\, \mathrm{d}t \geqslant \mu\gamma\lambda_{\max}^{-2} \int_0^T \boldsymbol{y}^{\mathrm{T}} \boldsymbol{y}\, \mathrm{d}t$$

assuming $\mu > 0$ and $\gamma > 0$, and $\lambda_{\max} = \max_i\{\lambda_i\}$.

The passivity theorem applied to Fig. 1 states that the negative feedback interconnection of a passive operator $\boldsymbol{G}$ and a strictly passive operator $\boldsymbol{H}$ is L_2-stable. Since $\boldsymbol{G}$ is LTI it can be described in the frequency domain by a transfer matrix $\mathbf{G}(s) = \mathrm{diag}\{G_i(s)\}$, $i = 1, 2, 3$. From the block diagram, it is clearly diagonal and

$$G_i(s) = \frac{\epsilon k_d s + \epsilon^2 k_p}{s^2 + \gamma_i'(\epsilon k_d s + \epsilon^2 k_p)}, \quad \gamma_i' = \frac{(1-\mu)\gamma}{\lambda_i^2} \tag{10}$$

It is well known that an LTI operator $\boldsymbol{G}$ is passive if its corresponding transfer matrix is positive real. Here, conditions will be established that render $G_i(s)$, hence $\mathbf{G}(s)$, strictly positive real (SPR), which is a slightly stronger condition. Since $G_i(s)$ is strictly proper, it is SPR if [**9**]:

(a) it is analytic in $\mathrm{Re}\{s\} \geqslant 0$;
(b) $\mathrm{Re}\{G_i(\mathrm{j}\omega)\} > 0, \ -\infty < \omega < \infty$;
(c) $\lim_{\omega\to\infty} \omega^2 \mathrm{Re}\{G_i(\mathrm{j}\omega)\} > 0$.

Clearly (a) is satisfied if

$$\gamma > 0, \quad k_d > 0, \quad k_p > 0, \quad \epsilon > 0, \quad \mu < 1 \tag{11}$$

It is easy to show that

$$Re\{G_i(\mathrm{j}\omega)\} = \frac{(\gamma_i' k_d^2 - k_p)\epsilon^2\omega^2 + \gamma_i'\epsilon^4 k_p^2}{(\gamma_i'^2 \epsilon^2 k_p - \omega^2)^2 + (\gamma_i' \epsilon k_d \omega)^2} \tag{12}$$

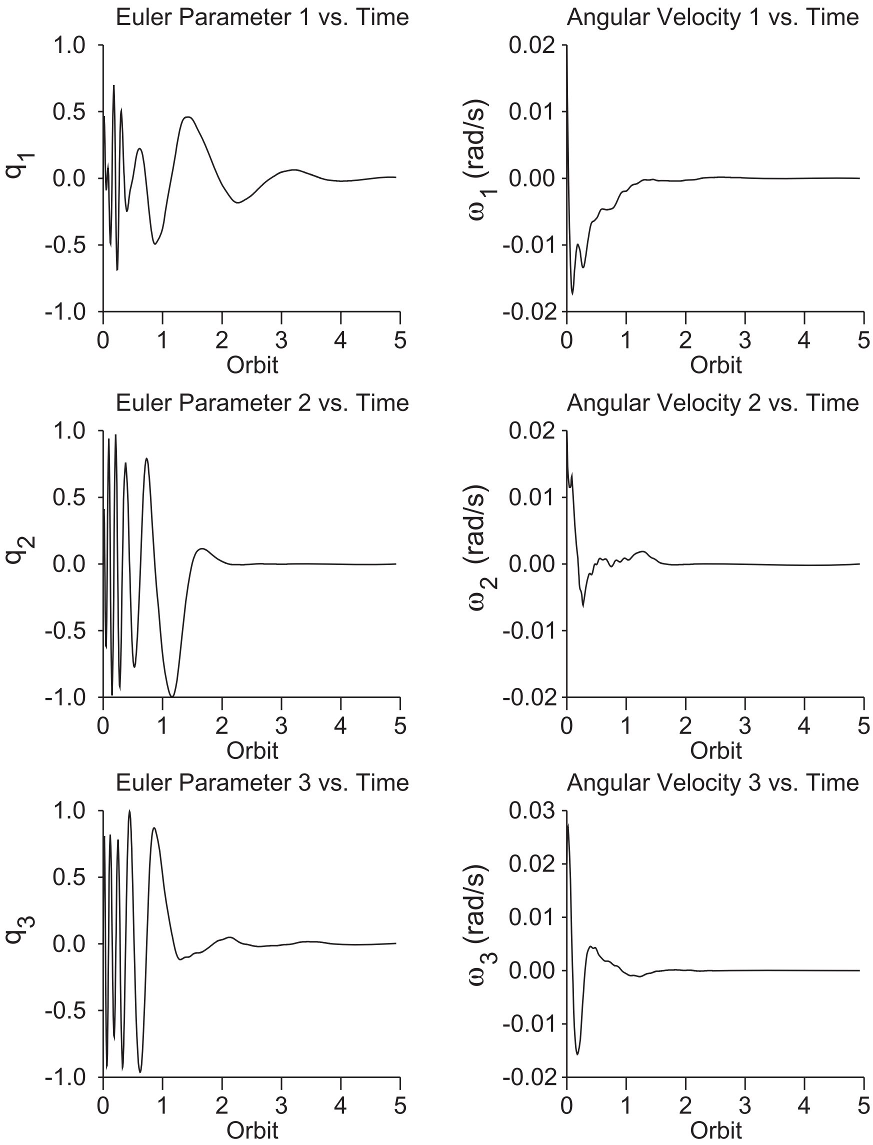

Fig. 2 Results for magnetic torque alone ($\epsilon = 0.001$, $\gamma = 0$)

and hence

$$\lim_{\omega \longrightarrow \infty} \omega^2 \mathrm{Re}\{G_\mathrm{i}(\mathrm{j}\omega)\} = (\gamma_\mathrm{i}'^2 k_\mathrm{d}^2 - k_\mathrm{p})\epsilon^2 \tag{13}$$

Therefore, a sufficient condition for (b) and (c) to be satisfied (assuming (11) is satisfied) is

$$\gamma_\mathrm{i}' k_\mathrm{d}^2 - k_\mathrm{p} > 0 \tag{14}$$

Letting $\mu \to 0$, this can be satisfied for $i = 1, 2, 3$ if

$$\gamma > \frac{k_\mathrm{p}\lambda_{\max}^2}{k_\mathrm{d}^2} \tag{15}$$

Note that if this is satisfied, there exists $\mu > 0$ so that (14) is satisfied for $i = 1, 2, 3$. It is concluded that if the conditions in equations (11) and (15) are satisfied, then the conditions of the passivity theorem are met and $\hat{\boldsymbol{d}} \in L_2 \Rightarrow \boldsymbol{y} \in L_2$. Using Laplace transforms, note that $\boldsymbol{\psi}(s) = \mathbf{M}(s)\boldsymbol{y}(s)$ where $\mathbf{M}(s) = (\epsilon k_\mathrm{d} s + \epsilon^2 k_\mathrm{p})^{-1}\mathbf{1}$. Since $\mathbf{M}(s) \in H_\infty$ and $s\mathbf{M}(s) \in H_\infty$, $\boldsymbol{y} \in L_2$ implies that $\boldsymbol{\psi} \in L_2$ and $\dot{\boldsymbol{\psi}} \in L_2$ and hence $\lim_{t\to\infty} \boldsymbol{\psi}(t) = \mathbf{0}$. Therefore, $\boldsymbol{\theta}(t) = \mathbf{E}\boldsymbol{\psi}(t) \to \mathbf{0}$ as $t \to \infty$. This complete the input–output stability treatment of equation (8).

Let us now turn to a Lyapunov-style treatment consistent with lemmas 1 and 2. Let $\mathbf{G}(s) = \mathbf{C}(s\mathbf{1} - \mathbf{A})^{-1}\boldsymbol{B}$ denote a minimal realization of $\boldsymbol{G}$ and let $\boldsymbol{x} = \mathrm{col}\{\boldsymbol{\psi}, \dot{\boldsymbol{\psi}}\}$ denote the corresponding state vector. Therefore, for $\hat{\boldsymbol{d}} = \mathbf{0}$, the block diagram in Fig. 1 can be realized as

$$\boldsymbol{y} = \mathbf{C}\boldsymbol{x}, \quad \dot{\boldsymbol{x}} = \mathbf{A}\boldsymbol{x} + \boldsymbol{B}\boldsymbol{v}, \quad \boldsymbol{v} = -[\boldsymbol{\Xi}(t) + \mu\gamma\boldsymbol{\Lambda}^{-2}]\boldsymbol{y} \tag{16}$$

Since $\mathbf{G}(s)$ is SPR, the Kalman–Yakubovich lemma guarantees the existence of $\mathbf{P} = \mathbf{P}^\mathrm{T} > \mathbf{O}$ and $\mathbf{Q} = \mathbf{Q}^\mathrm{T} >$

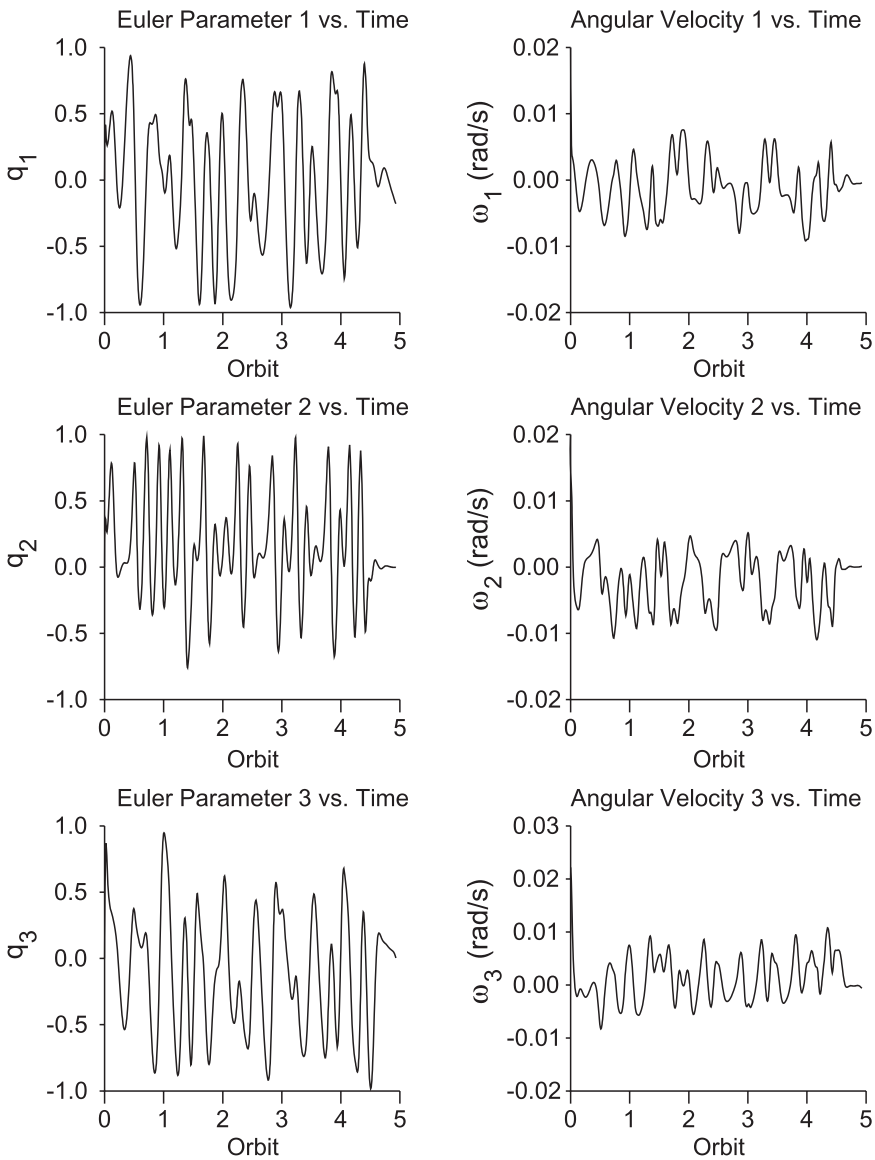

Fig. 3 Results for magnetic torque alone ($\epsilon = 0.005$, $\gamma = 0$)

$\mathbf{O}$ such that $\mathbf{PA} + \mathbf{A}^{\mathrm{T}}\mathbf{P} = -\mathbf{Q}$, $\mathbf{PB} = \mathbf{C}^{\mathrm{T}}$. Adopting $V = 1/2\boldsymbol{x}^{\mathrm{T}}\mathbf{P}\boldsymbol{x}$ as a Lyapunov function, it is easy to show that

$$\dot{V} = -\frac{1}{2}\boldsymbol{x}^{\mathrm{T}}\mathbf{Q}\boldsymbol{x} - \boldsymbol{y}^{\mathrm{T}}[\boldsymbol{\Xi}(t) + \mu\gamma\boldsymbol{\Lambda}^{-2}]\boldsymbol{y} \tag{17}$$

Hence, the system in equation (7) ($\boldsymbol{d} = \mathbf{0}$) is asymptotically stable and therefore so is that in equation (8). It is concluded that if the conditions in equations (11) and (15) are satisfied, then the system in equations (1), (2), (4), and (5) is locally asymptotically stable.

It is important to realize that unlike the purely magnetic situation covered by lemma 2, there is no scaling condition on ϵ. Hence, if the gain γ governing the three-axis actuation is sufficiently large, then the hybrid control scheme will be stable for any magnetic field.

As noted in the Introduction, magnetic torquers are often used for momentum dumping of reaction wheels. This is possible within this scheme since if the magnetic portion of the control law is removed (and used to generate an external torque for momentum dumping), the remaining part of the control (due to the reaction wheels) is globally asymptotically stable and input–output stable.

4 NUMERICAL EXAMPLE

Let us consider a rigid spacecraft with moment of inertia matrix $\mathbf{I} = \mathrm{diag}\{27, 17, 25\}\,\mathrm{kg \cdot m^2}$. It is in a circular Keplerian orbit with altitude 450 km and inclination 87°. The longitude of the ascending node and argument of latitude at $t = 0$ are zero. The right ascension of the Greenwich meridian is zero at $t = 0$.

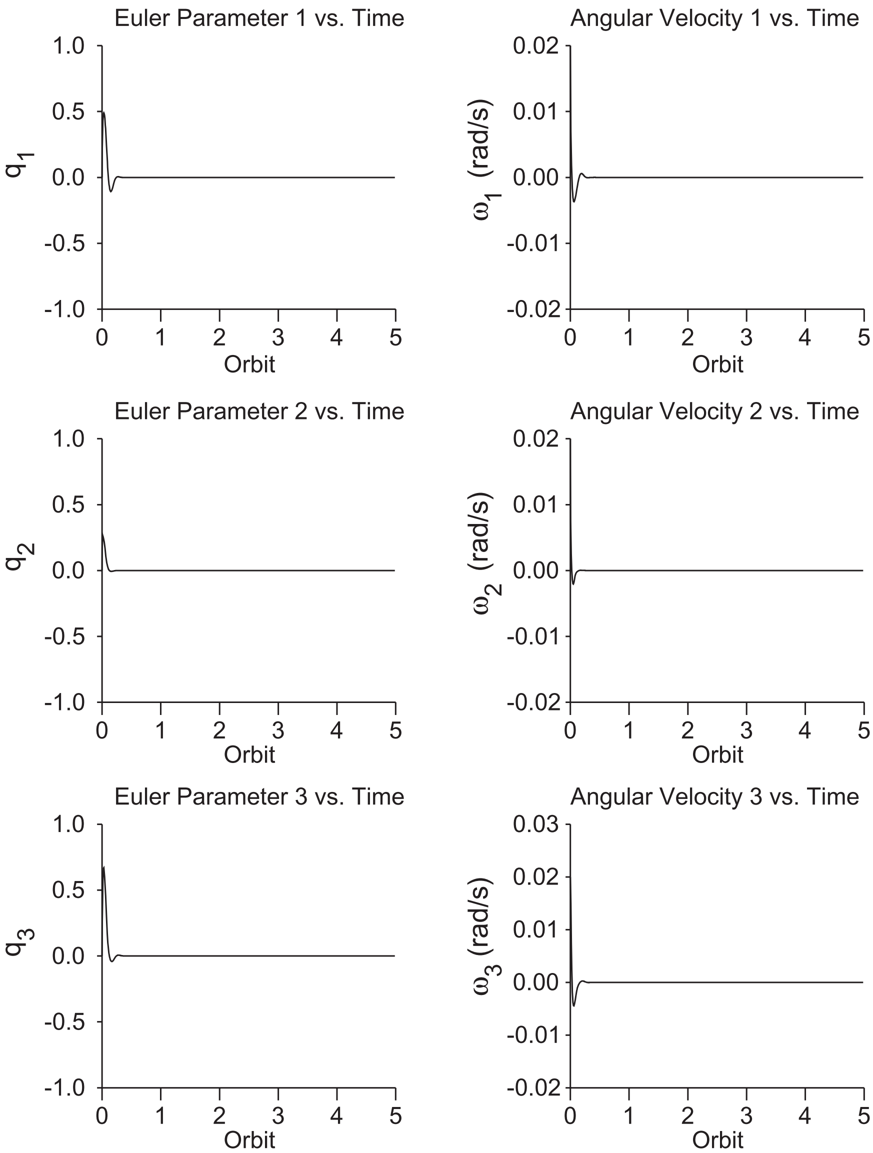

Fig. 4 Results for hybrid torque control ($\epsilon = 0.005$, $\gamma = 1.2$)

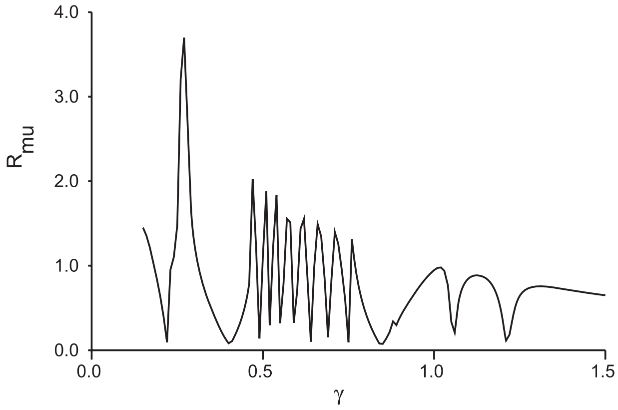

Fig. 5 Magnetic torque to three-axis torque ratio versus γ ($\epsilon = 0.005$)

The initial conditions are $\boldsymbol{q} = \boldsymbol{0}$, $q_4 = 1$, and $\omega_1 = \omega_2 = \omega_3 = 0.02$ rad/s. The initial gain selection is as follows

$$k_{\mathrm{d}} = 625\,\mathrm{kg}^2\,\mathrm{m}^4/\mathrm{s}, \quad k_{\mathrm{p}} = 625\,\mathrm{kg}^2\,\mathrm{m}^4/\mathrm{s}^2$$
$$\epsilon = 0.001 \tag{18}$$

The use of the magnetic controller alone (i.e. $\gamma = 0$) leads to the attitude and angular velocity histories shown in Fig. 2. Clearly, there is asymptotic stability. When ϵ is increased to 0.005, the resulting trajectories are shown in Fig. 3. In this case, the stability of the previous results has been lost, which demonstrates the existence of the limitation on gain size when using magnetic control alone.

For the above values of k_{d} and k_{p}, the critical value of γ predicted by equation (15) is 1.17. The simulation results for $\epsilon = 0.005$ and $\gamma = 1.2$ are given in Fig. 4. The addition of the three-axis actuation scheme has led to an asymptotically stable attitude equilibrium. Further simulation results show that for this value of ϵ, stability is achieved for $\gamma > 0.16$ demonstrating the sufficient but not necessary nature of the bound in equation (15).

Let us denote the magnetic torque by $\boldsymbol{\tau} = \boldsymbol{m}^{\times}\boldsymbol{B}_{\mathrm{b}}$ and recall that $\boldsymbol{u}$ is the three-axis control torque. Defining $\|\boldsymbol{u}\|_2 = \sqrt{\int_0^{5\mathrm{T}} \boldsymbol{u}^{\mathrm{T}}\boldsymbol{u}\,\mathrm{d}t}$ where T is the orbital period, the ratio $R_{\mathrm{mu}} = \|\boldsymbol{\tau}\|_2/\|\boldsymbol{u}\|_2$ is plotted against γ in Fig. 5. Interestingly, the curve is not monotonically decreasing but falls within an envelope that is.

5 CONCLUSIONS

A hybrid attitude control scheme consisting of magnetic torques produced by the geomagnetic field interacting with on-board torquing coils augmented with an independent three-axis actuation scheme has been considered. The limited gain margin of the magnetic scheme when used alone has been noted and shown to be alleviated by the suitable introduction of additional actuation from the three-axis scheme. A linear stability analysis has been presented using passivity concepts and minimal bounds on the three-axis control gains were obtained. Numerical simulations validated the concepts.

REFERENCES

1 **Silani, E.** and **Lovera, M.** Magnetic spacecraft attitude control: a survey and some new results. *Control Eng. Pract.*, 2005, **13**, 357–371.
2 **Lovera, M.** and **Astolfi, A.** Spacecraft attitude control using magnetic actuators. *Automatica*, 2004, **40**, 1405–1414.
3 **Lovera, M.** and **Astolfi, A.** Global magnetic attitude control of inertially pointing spacecraft. *J. Guid., Control Dyn.*, 2005, **28**(5), 1065–1067.
4 **Wen, J. T.-Y.** and **Kreutz-Delgado, K.** The attitude control problem. *IEEE Trans. Autom. Control*, 1991, **36**(10), 1148–1162.
5 **Hughes, P. C.** *Spacecraft attitude dynamics*, 1986 (Wiley, New York).
6 **Wertz, J.** *Spacecraft attitude determination and control*, 1978 (D. Reidel Publishing Co., Dordrecht, The Netherlands).
7 **Wie, B.** *Space vehicle dynamics and control*, 1998 (AIAA, Washington, DC).
8 **Desoer, C. A.** and **Vidyasagar, M.** *Feedback systems: input-output properties*, 1975 (Academic Press, New York).
9 **Ioannou, P.** and **Tao, G.** Frequency domain conditions for strictly positive real functions. *IEEE Trans. Autom. Control*, 1987, **32**, 53–54.